GEOPHYSICAL RESEARCH LETTERS, VOL. 20, NO. 11, PAGES 1083-1086, JUNE 7, 1993

THE 1992 LANDERS EARTHQUAKE SEQUENCE: EARTHQUAKE OCCURRENCE AND STRUCTURAL HETEROGENEITIES

Dapeng Zhao and Hiroo Kanamori
Seismological Laboratory, California Institute of Technology

Abstract. The June 28, 1992, Mw 7.3 Landers earthquake occurred in the southeastern Mojave Desert, California. Over 10,000 aftershocks of the earthquake were recorded by the Caltech-USGS Southern California Seismic Network (SCSN) in 1992. To investigate the relationship between complexities in the crustal structure and variations in seismicity, we have used a tomographic method to invert 145,098 *P* wave arrival times from 3740 Landers earthquake aftershocks and 1148 other events recorded by 60 permanent and temporary SCSN stations. We determined a detailed *P* wave tomographic image with a spatial resolution of about 5 km and relocated the hypocenters with the obtained 3-D velocity model. The results show a correlation between seismicity patterns and velocity patterns and a tendency for regions rich in seismicity to be associated with higher velocities. The higher velocity areas are considered to be strong and brittle parts of the fault zone, which are apt to generate earthquakes. In contrast, low velocity areas are probably more ductile and weaker, allowing aseismic slippage.

Introduction

The June 28, 1992, Mw 7.3 Landers earthquake occurred in the southeastern Mojave Desert, California, approximately 180 km east of Los Angeles (see Figure 1) and caused a surface rupture extending over a distance of more than 70 km. Near the epicenter, the surface displacement on the fault trace was approximately 3 meters; near the northern end of the fault, the displacement reached 6.7 meters [*Sieh et al.*, 1993]. This earthquake was the largest to occur in the contiguous United States since the Kern County, California, earthquake (Ms 7.7) in 1952.

More than 10,000 aftershocks of the Landers earthquake were recorded by the Caltech-USGS Southern California Seismic Network (SCSN) in 1992. In order to investigate the relationship between structural heterogeneities and variations in seismicity, we used a tomographic method to invert a large number of arrival times from the Landers earthquake aftershocks for the determination of a three-dimensional (3-D) crustal structure model beneath the aftershock area and accurate hypocentral locations of the aftershocks.

Data and Method

We selected 3740 aftershocks which are recorded by more than 9 stations and have reliable hypocentral locations. In order to have a good ray coverage of the study area (see Figure 1), we also selected 1148 earthquakes which occurred in the period from January 1981 to May 1992. All these earthquakes have more than 20 *P* wave arrival times. Figure 2 shows the epicentral distribution of the total 4888 events we selected, which are, on the whole, uniformly distributed in the study area.

Paper number 93GL01239
0094-8534/93/93GL-01239$03.00

Figure 3 shows the distribution of seismic stations used. Five temporary stations have been added to the permanent SCSN stations in this area since the beginning of July 1992 to locate the aftershocks more accurately. In total, we used 60 seismic stations in the present study.

The total number of *P* wave arrival times from the 4888 events is 153,759. In order to avoid the effects of the *Pn* velocity anisotropy [*Vetter and Minster*, 1981; *Hearn*, 1984], Moho depth variation [*Sung and Jackson*, 1992], and the velocity heterogeneities outside of the study area, we used only the arrival times with epicentral distances shorter than 180 km. Thus the number of data we actually used in the inversion is reduced to 145,098. The accuracy of arrival time picking is estimated to be about 0.1 s for most of the data.

We have used the tomographic method of *Zhao et al.* [1992] to analyze the selected arrival times. Although the conceptual approach of this method parallels that of *Aki and Lee* [1976], it has the following additional features. (1) It is adaptable to a velocity structure with discontinuities in complex geometry and with 3-D velocity variations in the model. We set up 3-D grid nodes in the model and take the velocities at the nodes as unknown parameters. (2) Travel times and ray paths are calculated by using an efficient 3-D ray tracing technique [*Zhao et al.*, 1992]. (3) Later arrivals of converted and reflected waves can be easily used in the inversion in addition to first *P* and *S* wave arrivals. (4) LSQR algorithm of *Paige and Saunders* [1982] is used for inversion, allowing a large number of data to be used to solve a large tomographic problem. (5) The nonlinear tomographic problem is solved by iteratively conducting linear inversions. In each iteration hypocentral parameters and velocity structure are determined simultaneously. For details of the method, see *Zhao et al.* [1992].

Result and Discussion

We took the *Kanamori and Hadley* [1975] model (Figure 3b in their paper) as the starting velocity model for the inversion. Their model was constructed by using accurate arrival times from large quarry blasts. The standard veloc-

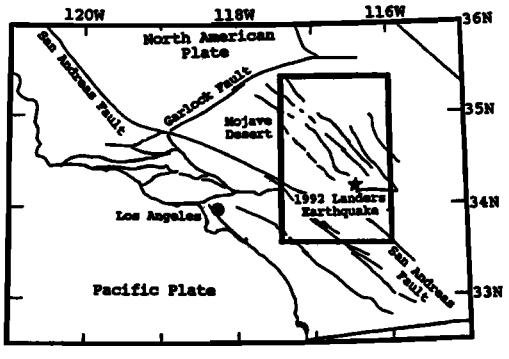

Fig. 1. *Southern California.* The box shows the present study area. Epicentral location of the June 28, 1992 Landers earthquake is shown by a star symbol. Major faults are shown by solid lines.

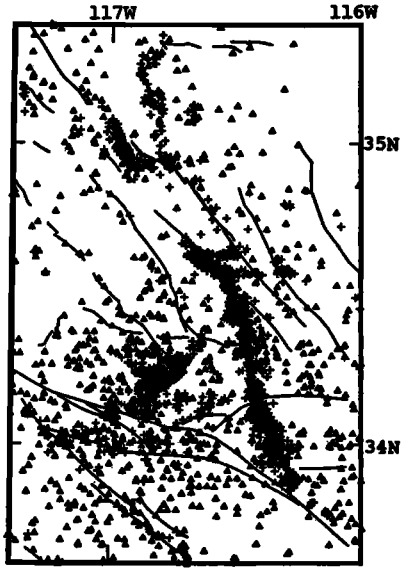

Fig. 2. Epicentral locations of the events used in the tomographic inversion. Cross symbols denote 3740 aftershocks of the Landers earthquake. Solid triangles denote 1148 other events. These 4888 events generated 145,098 arrival times which are used in the inversion.

ity model for the routine earthquake location by SCSN was derived from this structure.

We conducted a number of inversions by changing the grid spacing between grid nodes which are set up in the study area. Through resolution analyses for the different grid spacings, we found that a grid spacing of 5 km is adequate for the present data set and gives a reasonable result. A composite model for the P wave velocity structure was then constructed by averaging the results of a series of inversions for which the grid spacing was kept fixed but the grid as a whole was shifted systematically by 2 km in the latitude, longitude and depth directions. Typically the inversions achieved a 53% reduction of the data variance. The root mean square (RMS) travel time residual was reduced from 0.23 s before the inversions to 0.16 s after three iterations. The final RMS residual is approximately equal to the picking accuracy of the arrival times (0.1 s). We simultaneously determined 4888 x 4 hypocentral parameters and 2890 velocity perturbations for the grid nodes with hit counts (number of rays passing through the grid node) larger than 20. More than 99% of the grid nodes have hit counts greater than 80.

We also conducted detailed resolution and error analyses for the obtained 3-D velocity model using checkerboard-type methods [*Humphreys and Clayton*, 1988; *Zhao et al.*, 1992]. We found that the spatial resolution in and around the aftershock area is high (about 5 km), because the ray path coverage is very good there. The resolution for the fringe of the model, and for some areas in the lower part of the crust is slightly lower, about 6-9 km. The standard errors for the obtained velocity perturbations are estimated to be typically 1.5% (fractional error) for most part of the study area and 0.5-1% for the central part, suggesting that velocity variations greater than a few percent are significant.

Figure 4 shows the aftershocks of the Landers earthquake which occurred by the end of August, 1992 and the locations of cross sections to be considered below. Figure 5 shows depth distributions of the Landers earthquake aftershocks determined with the 1-D model of *Kanamori and Hadley* [1975] and the 3-D model of the present study, together with cross sections of fractional velocity perturbations along the profiles shown in Figure 4. The result along the northern segment of the fault zone of the Landers earthquake is shown in Figure 5a. A gap is visible at 3-4 km depth in the depth distribution of the aftershocks located with the 1-D model (see Figure 5a, top), it disappears in the distribution for the 3-D model (Figure 5a, middle). The two groups of aftershocks are separated by a prominent low velocity zone which extends from the surface to about 6 km. This low velocity structure is connected to a low velocity zone extending to about 18 km (Figure 5a, bottom). The northern group of aftershocks are surrounded by a very

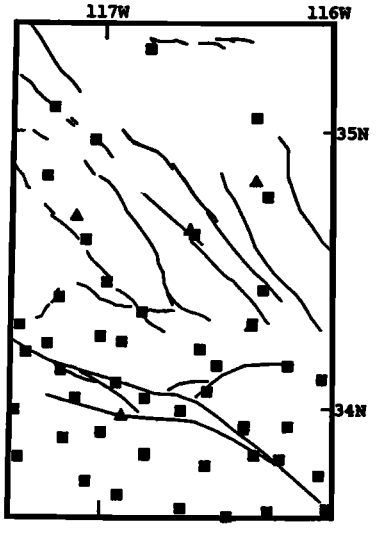

Fig. 3. Distribution of seismic stations of Caltech-USGS Southern California Seismic Network in the present study area. Solid squares and triangles denote permanent and temporary stations, respectively.

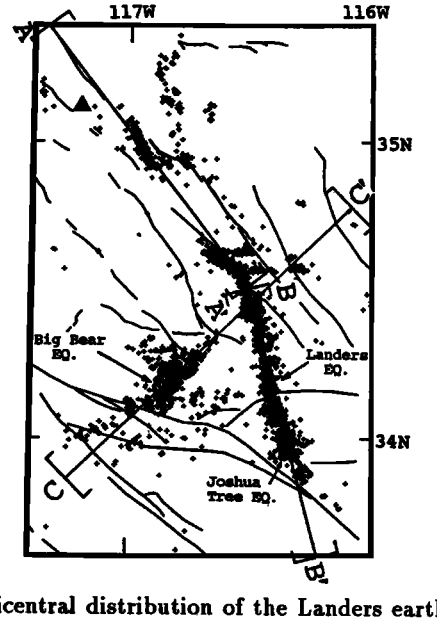

Fig. 4. Epicentral distribution of the Landers earthquake aftershocks which occurred from June 28 to August 31, 1992. Epicenters of the Landers earthquake mainshock, the Big Bear earthquake (June 28, 1992, Mw 6.3), and the Joshua Tree earthquake (April 23, 1992, Mw 6.2) are shown by star symbols. Locations of the three cross sections in Figure 5 are shown. The solid triangle denotes the Black Mountain volcanic center.

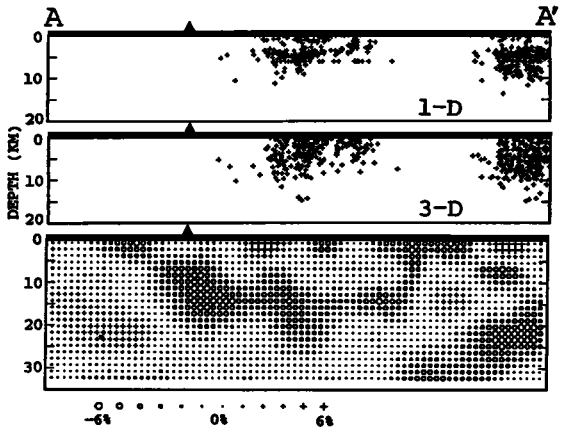

Fig. 5 (a). Depth distribution of the aftershocks along AA' profile (see Figure 4) determined with the 1-D velocity model of *Kanamori and Hadley* [1975] (*top*) and with the 3-D velocity model of this study (*middle*). (*Bottom*) Vertical cross section of fractional P wave velocity perturbation (in %) along AA' profile. Cross and circle symbols denote high and low velocities, respectively. A solid triangle denotes the Black Mountain volcanic center. The perturbation scale is shown below the figure.

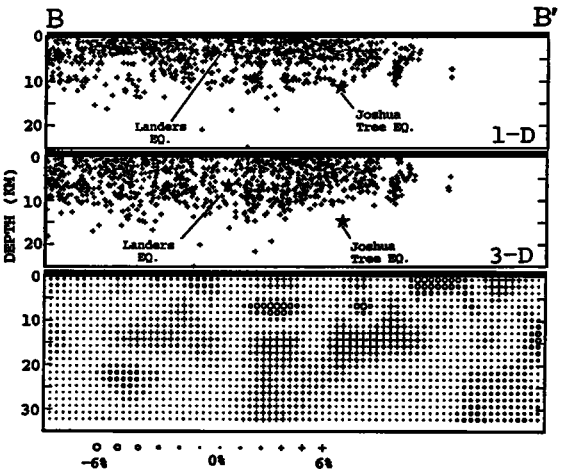

Fig. 5 (b). The same as Figure 5 (a) but along profile BB'. Hypocenters of the Landers earthquake mainshock and the Joshua Tree earthquake determined with the 1-D and 3-D models are shown by stars.

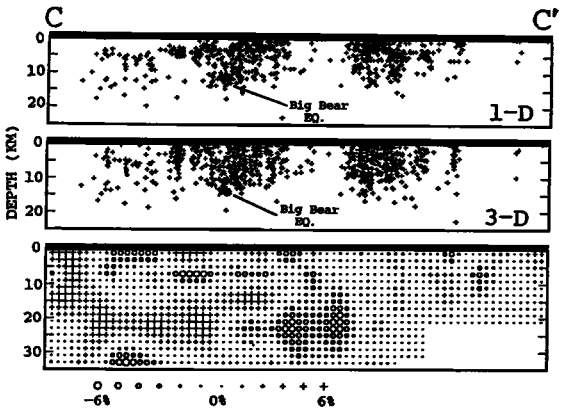

Fig. 5 (c). The same as Figure 5 (a) but along profile CC'. Hypocenters of the Big Bear earthquake determined with the 1-D and 3-D models are shown by stars.

large low velocity zone beneath them. The Black Mountain volcanic center is underlain by the northern end of the large low velocity zone. The velocity structure in and around the southern group of aftershocks is more complex. The velocity is high from 0 to 5 km and becomes low in the deeper area.

The depth distribution of the aftershocks which occurred in the southern segment of the Landers earthquake fault zone and the velocity distribution are shown in Figure 5b. The seismicity is terminated in the south where a shallow low velocity zone exists. The low velocity zone extends from the surface to a depth of about 5 km. The Landers earthquake mainshock is located at 1.1 km depth by routine processing of SCSN with the 1-D model; we relocated it at 7.0 km depth using the 3-D velocity model. The RMS travel time residual for the relocated hypocenter is considerably reduced. The difference between the epicentral locations determined with the two models is small, less than 1 km.

We can also see in Figure 5b that, at the depth range of 5 to 10 km, the velocity is low just south of the Landers earthquake mainshock hypocenter and high north of it. Note that the rupture propagated northward from the epicenter [*Kanamori et al.*, 1992]. Also shown in Figure 5b is the hypocenter of the 23 April 1992, Mw 6.2 Joshua Tree earthquake, which can be considered as a foreshock of the Landers earthquake [*Sieh et al.*, 1993]. It is located at 12.4 km depth by SCSN and relocated at 15.2 km depth by the present study. The hypocenter of the Joshua Tree earthquake is located in a large high velocity area.

Figure 5c shows the result along a profile passing through the Big Bear aftershock region. The focal depth of the Big Bear earthquake determined by routine processing is 12.2 km, while the relocated focal depth in the 3-D model is 14.4 km. The hypocenter of the Big Bear earthquake is also located in a high velocity zone (see Figure 5c). In the cross section, we can also see that the velocities between the Landers aftershock sequence and the Big Bear aftershock sequence are generally low from the surface to the bottom of the crust.

The relocated hypocenters with the 3-D velocity model are, on average, 2-3 km deeper than those determined by the routine processing. *Zhao and Kanamori* [1992] determined a P wave tomographic image of the entire southern California. Main features of the image determined in the present study are consistent with those determined by *Zhao and Kanamori* [1992], though there are some minor differences in the small scale features due to the different resolution scales (25 km in *Zhao and Kanamori* [1992] and 5 km in the present study).

As described above, the seismic rupture zones in the upper crust around the Landers earthquake fault zone are generally imaged with high velocity. Near the end of the rupture zones low-velocity structures are usually seen. Similar results have been reported by *Lees* [1990], *Lees and Malin* [1990], *Michael and Eberhart-Phillips* [1991], and *Nicholson and Lees* [1992] for the Parkfield, Loma Prieta, Morgan Hills, Coalinga, and North Palm Springs earthquakes, though details are different for each earthquake. Although it is still unclear how seismic velocity is related to earthquake rupture zones, higher velocity areas are generally considered to be associated with more brittle and competent parts of the crust which sustain seismogenic stress. In contrast, lower velocity regions may represent the regions of either higher degree of fracture, high fluid pressure, or higher temperatures where deformation is more likely to be aseismic. Compositional variations may be also responsible for velocity variations.

If this correlation generally holds, it has an important implication that seismic rupture zones are fixed in space

throughout many earthquake sequences. To obtain more definitive pictures, however, higher resolution tomographic models are required.

Conclusions

We have used a large number of arrival times from the 1992 Landers earthquake aftershocks and other events to investigate the crustal structure in and around the aftershock region. A detailed *P* wave tomographic image is determined with a spatial resolution of approximately 5 km and hypocentral locations are improved with the obtained 3-D velocity model. The results show a correlation between seismicity patterns and velocity patterns and a tendency for regions rich in seismicity to be associated with higher velocities. We consider that the high velocity areas are probably brittle and strong parts along the fault zone, which are responsible for generating the mainshock and aftershocks; while low velocity areas probably have a weak and ductile feature which may not effectively generate earthquakes. This result suggests the possibility that earthquake occurrence is closely related to the *in situ* material heterogeneities.

Acknowledgements. We appreciate the helpful discussions with D. L. Anderson, T. Heaton, K. Aki and E. Humphreys. D. Wald and two anonymous referees critically read the manuscript and gave us helpful comments, which improved the manuscript. The first author (DZ) was supported by the Southern California Earthquake Center (SCEC) and this is SCEC Publication No. 27. This work was partially supported by a National Science Foundation grant, EAR-92-04748. Contribution No. 5247, Division of Geological and Planetary Sciences, California Institute of Technology.

References

Aki, K. and W. H. K. Lee, Determination of three-dimensional velocity anomalies under a seismic array using first P arrival times from local earthquakes, 1, A homogeneous initial model, *J. Geophys. Res.*, *81*, 4381-4399, 1976.

Hearn, T. M., Pn travel times in southern California, *J. Geophys. Res.*, *89*, 1843-1855, 1984.

Humphreys, E. and R. W. Clayton, Adaptation of back projection tomography to seismic travel time problems, *J. Geophys. Res.*, *93*, 1073-1085, 1988.

Kanamori, H. and D. Hadley, Crustal structure and temporal velocity change in Southern California, *Pure and Appl. Geophys.*, *113*, 257-280, 1975.

Kanamori, H., H. Thio, D. Dreger, E. Hauksson, and T. Heaton, Initial investigation of the Landers, California, earthquake of 28 June 1992 using TERRAscope, *Geophys. Res. Lett.*, *19*, 2267-2270, 1992.

Lees, J. M., Tomographic P-wave velocity images of the Loma Prieta earthquake asperity, *Geophys. Res. Lett.*, *17*, 1433-1436, 1990.

Lees, J. M. and P. E. Malin, Tomographic images of P-wave velocity variations at Parkfield, California, *J. Geophys. Res.*, *95*, 21793-21804, 1990.

Michael, A. J. and D. Eberhart-Phillips, Relations among fault behavior, subsurface geology, and three-dimensional velocity models, *Science*, *253*, 651-654, 1991.

Nicholson, C. and J. M. Lees, Travel-time tomography in the northern Coachella Velley using aftershocks of the 1986 M 5.9 North Palm Springs earthquake, *Geophys. Res. Lett.*, *19*, 1-4, 1992.

Paige, C. C. and M. A. Saunders, LSQR: An algorithm for sparse linear equations and sparse least squares, *ACM Trans. Math. Software*, *8*, 43-71, 1982.

Sieh, K., L. Jones, E. Hauksson, K. Hudnut, D. Eberhart-Phillips, T. Heaton, S. Hough, K. Hutton, H. Kanamori, A. Lilje, S. Lindvall, S. McGill, J. Mori, C. Rubin, J. Spotila, J. Stock, H. Thio, J. Treiman, B. Wernicke, J. Zachariasen, Near-field investigations of the Landers earthquake sequence, April to July 1992, *Science*, *260*, 171-176, 1993.

Sung, L. Y. and D. D. Jackson, Crustal and uppermost mantle structure under southern California, *Bull. Seism. Soc. Am.*, *82*, 934-961, 1992.

Vetter, U. and J. B. Minster, Pn velocity anistropy in southern California, *Bull. Seism. Soc. Am.*, *71*, 1511-1530, 1981.

Zhao, D., A. Hasegawa, and S. Horiuchi, Tomographic imaging of P and S wave velocity structure beneath northeastern Japan, *J. Geophys. Res.*, *97*, 19909-19928, 1992.

Zhao, D. and H. Kanamori, P-wave image of the crust and uppermost mantle in southern California, *Geophys. Res. Lett.*, *19*, 2329-2332, 1992.

H. Kanamori and D. Zhao, Seismological Laboratory 252-21, California Institute of Technology, Pasadena, CA 91125.

(Received: February 11, 1993;
accepted: March 30, 1993.)